Electronic Supporting Information

Pyridine-3,5-dicarbonitrile cored emitters with short delayed fluorescence lifetimes of about 1.5 μs: orange-red TADF based OLEDs with very slow efficiency roll-offs at high luminance

Zhanxiang Chen,[a] Zhongbin Wu,[c] Fan Ni,[a] Cheng Zhong,[a] Weixuan Zeng,[a] Danqing Wei,[a] Kebin An,[a] Dongge Ma[c,d] and Chuluo Yang*[a,b]*

Z. Chen, F. Ni, W. Zeng, Prof. C. Zhong, D. Wei, K. An, and Prof. C. Yang

Hubei Key Lab on Organic and Polymeric Optoelectronic Materials, Department of Chemistry, Wuhan University, Wuhan 430072, P. R. China. E-mail: clyang@whu.edu.cn

Shenzhen Key Laboratory of Polymer Science and Technology, College of Materials Science and Engineering, Shenzhen University, Shenzhen 518060, P. R. China.

Dr. Z. Wu and Prof. D. Ma

State Key Laboratory of Polymer Physics and Chemistry, Changchun Institute of Applied Chemistry, Chinese Academy of Sciences, Changchun 130022, P. R. China.

State Key Laboratory of Luminescent Materials and Devices, Institute of Polymer Optoelectronic Materials and Devices, South China University of Technology, Guangzhou 510640, P. R. China. E-mail: msdgma@scut.edu.cn

General information

All oxygen- and moisture-sensitive manipulations were carried out under an inert atmosphere. All the chemicals were purchased from commercial sources and used as received unless stated otherwise. Toluene was refluxed over Na/K alloy and distilled under dry argon. Synthesized compounds were subject to purification by temperature-gradient sublimation in high vacuum before used in subsequent studies. The 400 MHz ^{1}H and 100 MHz ^{13}C NMR spectra were recorded on a MERCUYR-VX300 spectrometer using $CDCl_3$ as solvent and tetramethylsilane (TMS) as an internal reference. HRMS spectra was measured by LCQ-Orbitrap Elite (Thermo-Fisher Scientific, Waltham, MA, USA) mass spectrometer. UV-Vis absorption spectra were recorded on a Shimadzu UV-2700 recording spectrophotometer. Photoluminescence (PL) spectra were recorded on a Hitachi F-4600 fluorescence spectrophotometer. Phosphorescence spectra of thin films were conducted at 77K. Thermogravimetric analysis (TGA) was recorded on a NEZSCH STA 449C instrument under nitrogen atmosphere at a heating rate of 10ºC/min from 25ºC to 650ºC. The temperature of degradation (T_d) was correlated to a 5% weight loss. The glass transition temperature (T_g) was determined from the second heating scan at a heating rate of 10ºC min^{-1} from -60 to 235ºC. Cyclic voltammetry (CV) was carried out in nitrogen-purged tetrahydrofuran or acetonitrile (reduction scan) or dichloromethane (oxidation scan) at room temperature with a CHI voltammetric analyzer. Tetrabutylammonium hexafluorophosphate (0.1 M) was used as the supporting electrolyte. The conventional three-electrode configuration consisted of a platinum working electrode, a platinum

wire auxiliary electrode and an Ag wire pseudo-reference electrode with ferrocenium-ferrocene (Fc^+/Fc) as the internal standard. Cyclic voltammograms were obtained at scan rate of 100 mV/s. Formal potentials were calculated as the average of cyclic voltammetric anodic and cathodic peaks. The HOMO energy levels of the compounds were calculated according to the formula: $-[4.8 + (E_{1/2(ox/red)} - E_{1/2(Fc/Fc^+)})]$ eV. The LUMO energy levels of the compounds were calculated according to the formula: $-[4.8 - (E_{1/2(red/ox)} - E_{1/2(Fc/Fc^+)})]$ eV. The onset potential was determined from the intersection of two tangents drawn at the rising and background current of the cyclic voltammogram. The PL lifetimes were measured by a single photon counting spectrometer from Edinburgh Instruments (FLS920) with a Picosecond Pulsed UV-LASTER (LASTER377) as the excitation source. The samples were placed in a vacuum cryostat chamber with the temperature control. The solid state absolute PLQYs were measured on a Quantaurus-QY measurement system (C9920-02, Hamamatsu Photonics) equipped with a calibrated integrating sphere in the host of CBP (10 wt%) and all the samples were excited at 330 nm. During the PLQY measurements, the integrating sphere was purged with pure and dry argon to maintain an inert environment. The ground state molecular structures were optimized at the B3LYP/6-31g(d) level of theory; the S_1 and T_1 geometries were optimized via time-dependent DFT (TDDFT) at the same level of theory. Energy gaps between first singlet state (S_1) and triplet state (T_1) were calculated using the TD-LC-ωPBE/6-31g(d) level of theory on the optimized geometry. In addition, the overlaps between the hole and electron density distributions in the S_1 and T_1 states were estimated by the Multiwfn code.

X-Ray Structural Analysis

The single crystal of PXZ-PCN and bis-PXZ-PCN were achieved from solvent diffusion method from n-hexane/trichloromethane mixed solutions. Single-crystal X-ray-diffraction data were obtained from a Bruker APEX2 Smart CCD diffractometer through using MoKα radiation (λ = 0.71073 Å) with a ω/2θ scan mode at 296 K. Structures of the crystals were solved by direct methods using the APEX2 software. None-hydrogen atoms were refined anisotropically by full-matrix least-squares calculations on F^2 using APEX2, while the hydrogen atoms were directly introduced at calculated position and refined in the riding mode. Drawings were produced using Mercury-3.3. CCDC-1821566 (PXZ-PCN) and CCDC-1821567 (bis-PXZ-PCN) contains supplementary crystallographic data. These data can be obtained free of charge from the Cambridge Crystallographic Data Centre via https://www.ccdc.cam.ac.uk/structures/.

Device Fabrication and Measurement

The electron-injection material of LiF was purchased from Sigma-Aldrich and used as received. The hole-transporting material of 4,4'-(cyclohexane-1,1-diyl)bis(N,N-di-p-tolylaniline) (TAPC), electron blocking material of 1,3-carbazol-benzene (mCP), host material of 4,4'-di(9H-carbazol-9-3yl)-1,1'-biphenyl (CBP) and electron transport material of 4,7-diphenyl-1,10-phenanthroline (Bphen) were purchased from Luminescence Technology Corporation and used as received. Patterned indium tin-

oxide (ITO)-coated glass substrates were cleaned with a standard regiment of deionized water, acetone and methanol inside an ultrasonic bath. After UV ozone treatment, the substrates were transferred to the vacuum chamber at a bass pressure of 10^{-5} Pa. Hole-injecting material MoO_3 (10 nm) and hole-transporting material TAPC (50 nm) were gradually deposited onto the ITO substrates, followed by an electron-blocking material mCP (10 nm), an emissive layer (20 nm) and electron-transporting material Bphen (45 nm). Finally, a cathode composed of LiF and Al was sequentially deposited. The current density-voltage-luminance (*J*-V-L) characteristics were measured using a HP4140B picoammeter and a Minolta LS-110 luminance meter. The EL spectra was collected by an USB2000-UV-vis Miniature Fiber Optic Spectrometer. All measurements were carried out in an ambient atmosphere and at room temperature.

Synthesis of PXZ-PCN, bis-PXZ-PCN and tri-PXZ-PCN

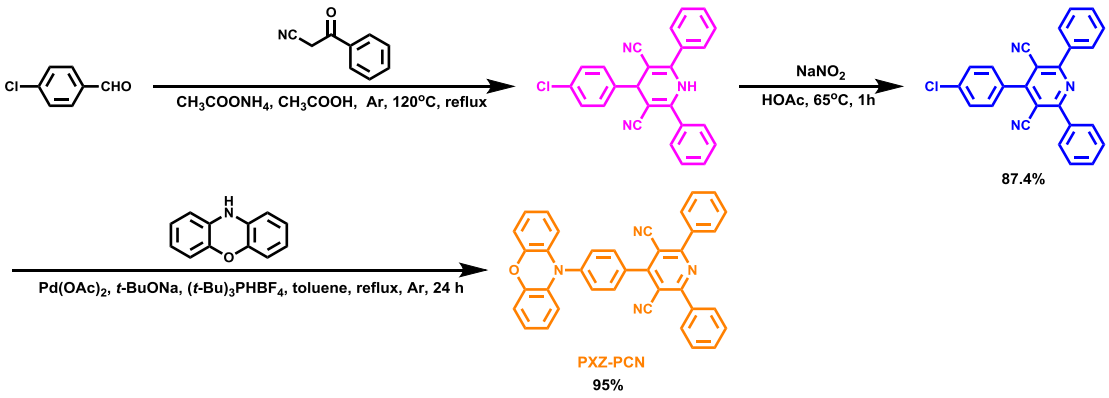

Scheme 1 Synthetic routes for PXZ-PCN.

Synthesis of 4-(4-chlorophenyl)-2,6-diphenylpyridine-3,5-dicarbonitrile

A solution of 3-oxo-3-phenylpropanenitrile (2.54 g, 17.5 mmol), 4-chlorobenzaldehyde (0.98 g, 7 mmol) and ammonium acetate (5.39 g, 70 mmol) in 175 ml of glacial acetic

acid was heated for 12 h at 120ºC under argon atmosphere. After 12 h, sodium nitrite (4.83 g, 70 mmol) was added in portions to the suspension under stirring at 65ºC. The mixture was stirred for another 1 h at the same temperature. After cooled down to room temperature, the mixture was then diluted with 700 mL ice-water mixture and neutralized with ammonia. The precipitate was filtered off and washed with water to afford 4-(4-chlorophenyl)-2,6-diphenylpyridine-3,5-dicarbonitrile as white powder (3.29 g, yield: 87.4%). ^{1}H NMR ($CDCl_3$, 400 MHz) δ (ppm): 7.55-7.63 (m, 10H), 8.06-8.08 (m, 4H). ^{13}C NMR ($CDCl_3$, 100 MHz) δ (ppm): 105.8, 115.8, 128.9, 129.6, 129.7, 130.3, 131.6, 131.9, 136.2, 137.7, 163.4. HRMS (ESI): m/z $[M+H]^+$ calcd for $C_{25}H_{15}ClN_3^+$: 392.0949; found: 392.0954.

Synthesis of 4-(4-(10*H*-phenoxazin-10-yl)phenyl)-2,6-diphenylpyridine-3,5-dicarbonitrile (PXZ-PCN)

4-(4-chlorophenyl)-2,6-diphenylpyridine-3,5-dicarbonitrile (1.37 g, 3.5 mmol), phenoxazine (0.77 g, 4.2 mmol), sodium tert-butoxide (404 mg, 4.2 mmol), palladium (II) acetate (16 mg, 0.07 mmol) and tri-tert-butylphosphine tetrafluoroborate (61 mg, 0.21 mmol) were added to a dry two-necked flask equipped with a magnetic stir bar and a condenser. The flask was then evacuated and backfilled with argon, this evacuation and backfill procedure was repeated twice. Then 35 mL toluene was added under argon atmosphere. The mixture was then stirred under reflux at 110ºC for 24 h. As the mixture was cooled down to room temperature, the reaction solution was transferred into a separatory funnel and then neutralized with anhydrous sodium sulfate. After filtration and concentration under reduced pressure, the crude product was

purified by column chromatography with dichloromethane/petroleum ether (v/v=1/1) as eluent to give the title compound as orange powder (1.752 g, yield: 95%). The resulting product was further purified by recrystallizing from a mixture of chloroform/hexane. Finally, this material was purified by sublimation under reduced pressure for OLED fabrication. ^{1}H NMR ($CDCl_3$, 400 MHz) δ (ppm): 6.05 (d, J = 8.0 Hz, 2H), 6.64-6.75 (m, 6H), 7.57-7.65 (m, 8H), 7.86 (d, J = 8.0 Hz, 2H), 8.11 (d, J = 8.0 Hz, 4H). ^{13}C NMR ($CDCl_3$, 100 MHz) δ (ppm): 105.8, 113.5, 115.7, 115.8, 121.9, 123.5, 128.9, 129.6, 131.6, 131.8, 133.7, 133.8, 136.3, 141.7, 144.0, 159.5, 163.4. HRMS (ESI): m/z $[M+Na]^+$ calcd for $C_{37}H_{22}N_4NaO^+$: 561.1691; found: 561.1658.

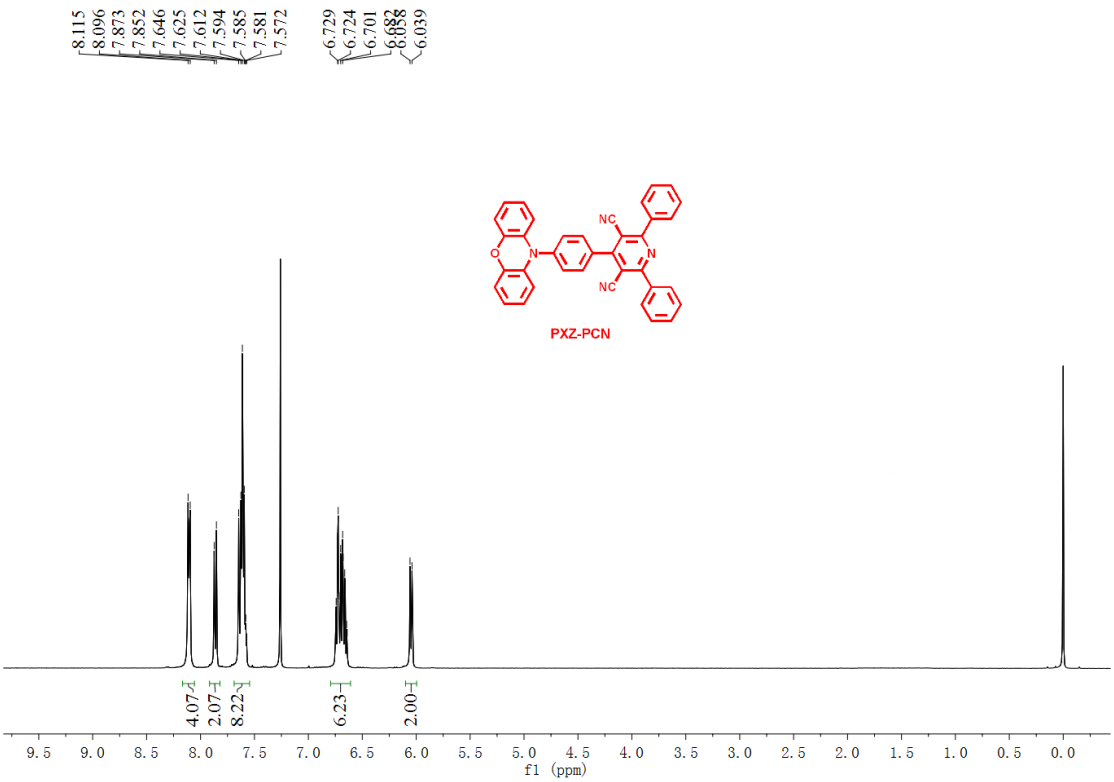

Figure S1. ^{1}H NMR spectrum of PXZ-PCN in $CDCl_3$ (400 MHz, 25 °C).

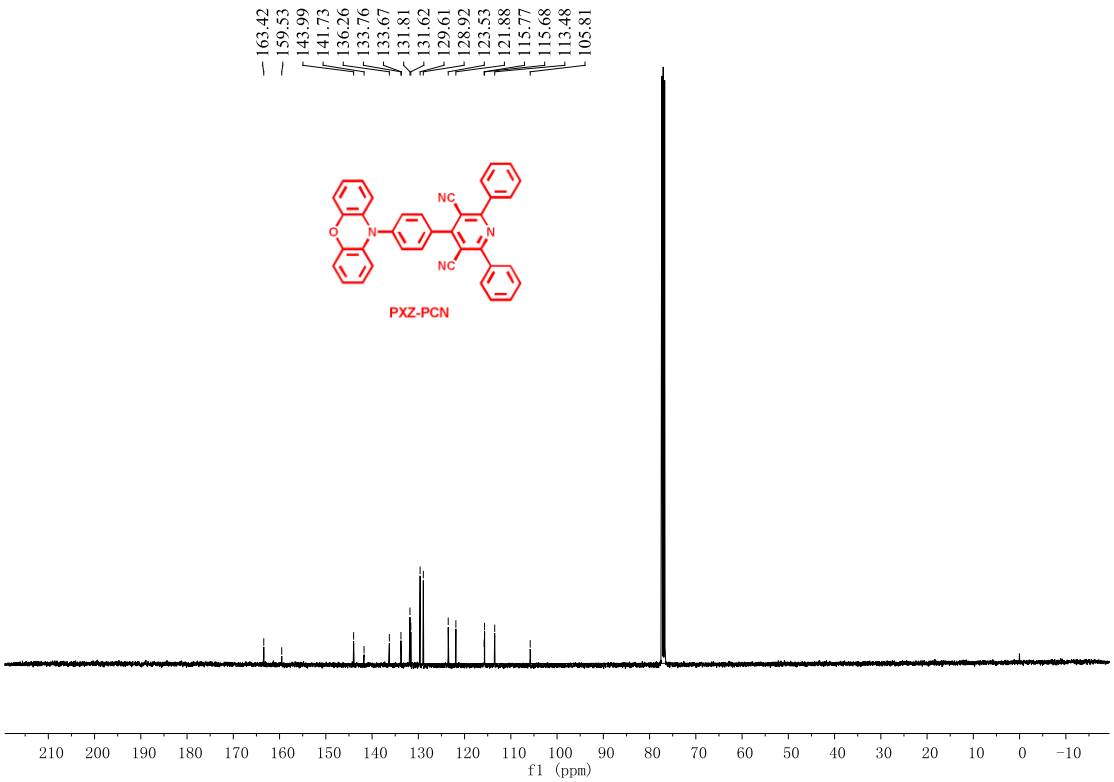

Figure S2. ^{13}C NMR spectrum of PXZ-PCN in $CDCl_3$ (100 MHz, 25 °C).

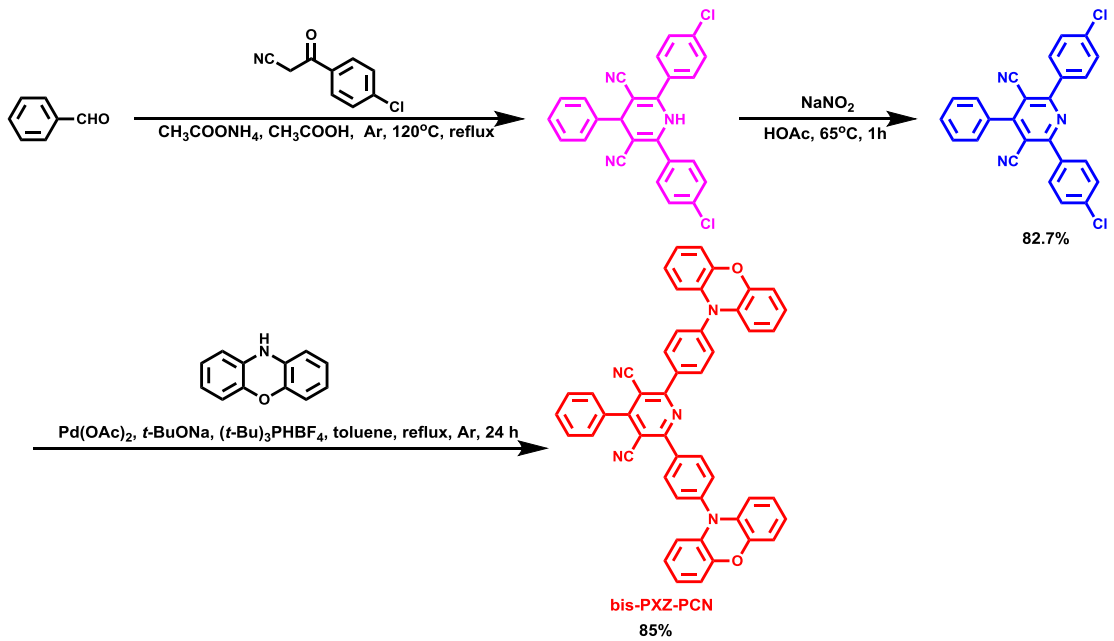

Scheme 2 Synthetic routes for bis-PXZ-PCN.

Synthesis of 2,6-bis(4-chlorophenyl)-4-phenylpyridine-3,5-dicarbonitrile

A mixture of 3-(4-chlorophenyl)-3-oxopropanenitrile (0.86 g, 4.8 mmol), benzaldehyde (0.21 g, 2 mmol) and ammonium acetate (1.54 g, 20 mmol) in 50 ml of glacial acetic acid was heated for 12 h at 120^{o}C under argon atmosphere. After 12 h, sodium nitrite (1.38 g, 20 mmol) was added in portions to a suspension under stirring at 60-70^{o}C. The mixture was stirred for 1 h at the same temperature. After cooled down to room temperature, the mixture was then diluted with 200 mL ice-water mixture, and neutralized with ammonia. The precipitate was filtered off and wash with water to afford 2,6-bis(4-chlorophenyl)-4-phenylpyridine-3,5-dicarbonitrile as white powder (0.70 g, yield: 82.7%). ^{1}H NMR ($CDCl_3$, 400 MHz) δ (ppm): 7.54-7.65 (m, 9H), 8.02-8.04 (m, 4H). ^{13}C NMR ($CDCl_3$, 100 MHz) δ (ppm): 106.0, 115.6, 128.8, 129.2, 129.3, 130.9, 131.3, 133.3, 134.5, 138.1, 162.1. HRMS (ESI): m/z $[M+H]^+$ calcd for $C_{25}H_{14}Cl_2N_3^+$: 426.0559; found: 426.0558.

Synthesis of 2,6-bis(4-(10*H*-phenoxazin-10-yl)phenyl)-4-phenylpyridine-3,5-dicarbonitrile (bis-PXZ-PCN)

2,6-bis(4-chlorophenyl)-4-phenylpyridine-3,5-dicarbonitrile (0.64 g, 1.5 mmol), phenoxazine (0.66 g, 3.6 mmol), sodium tert-butoxide (346 mg, 3.6 mmol), palladium (II) acetate (13 mg, 0.06 mmol) and tri-tert-butylphosphine tetrafluoroborate (52 mg, 0.18 mmol) were added to a dry two-necked flask equipped with a magnetic stir bar and a condenser. The flask was then evacuated and backfilled with argon, this evacuation and backfill procedure was repeated twice. Then 15 mL toluene was added under argon atmosphere. The mixture was then stirred under reflux at 110^{o}C for 24 h. As the mixture was cooled down to room temperature, the reaction solution was

transferred into a separatory funnel and then neutralized with anhydrous sodium sulfate. The organic phase was dried over anhydrous sodium sulfate. After filtration and concentration under reduced pressure, the crude product was purified by column chromatography with dichloromethane/petroleum ether (v/v=1/1) as eluent to give the title compound as red powder (1.18 g, yield: 86%). The resulting product was further purified by recrystallizing from a mixture of chloroform/hexane. Finally, this material was purified by sublimation under reduced pressure for OLED fabrication. ^{1}H NMR ($CDCl_3$, 400 MHz) δ (ppm): 6.05 (d, J = 8.0 Hz, 4H), 6.61-6.74 (m, 12H), 7.60 (d, J = 12.0 Hz, 4H), 7.68 (m, 5H), 8.35 (d, J = 8.0 Hz, 4H). ^{13}C NMR ($CDCl_3$, 100 MHz) δ (ppm): 106.4, 113.5, 115.66, 115.74, 121.9, 123.4, 128.9, 129.4, 131.4, 132.4, 133.3, 133.7, 136.1, 142.3, 144.0, 160.9, 162.2. HRMS (ESI): m/z $[M+H]^+$ calcd for $C_{49}H_{30}N_5O_2^+$: 720.2394; found: 720.2398.

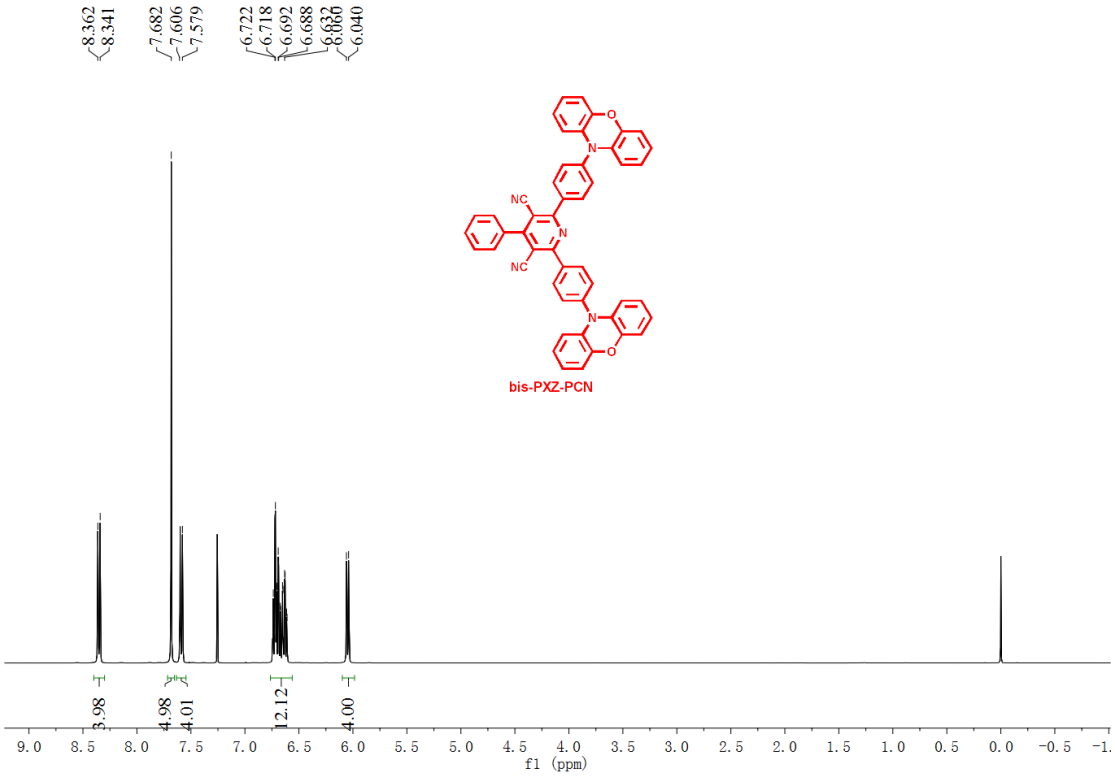

Figure S3. ^{1}H NMR spectrum of bis-PXZ-PCN in $CDCl_3$ (400 MHz, 25 °C).

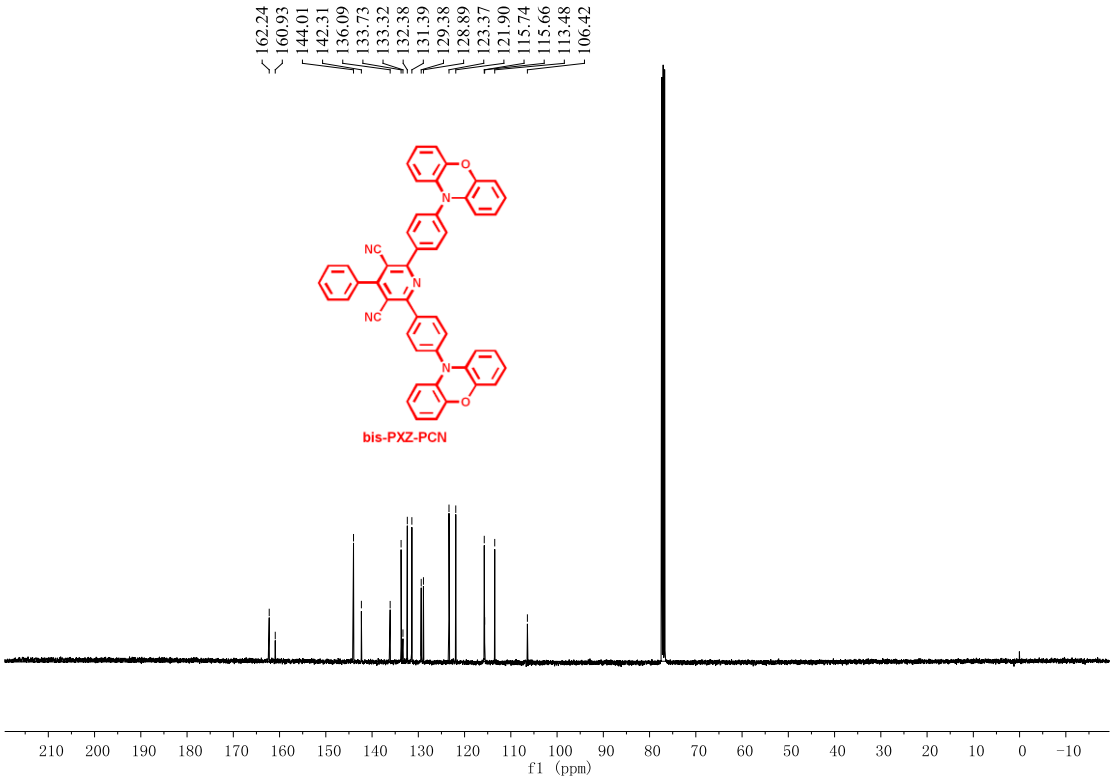

Figure S4. ^{13}C NMR spectrum of bis-PXZ-PCN in $CDCl_3$ (100 MHz, 25 °C).

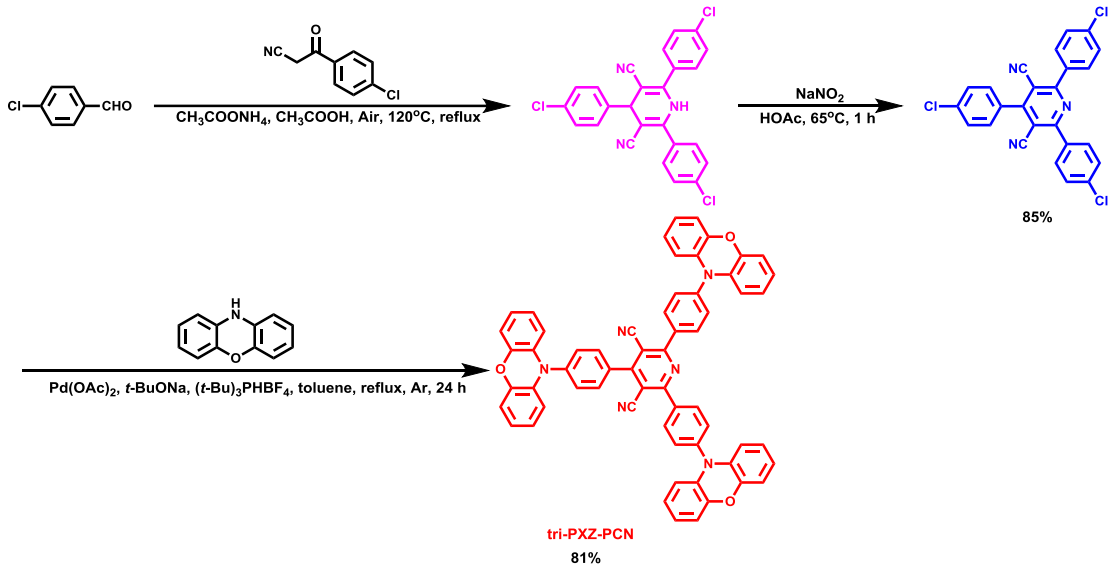

Scheme 3 Synthetic routes for tri-PXZ-PCN.

Synthesis of 2,4,6-tris(4-chlorophenyl)pyridine-3,5-dicarbonitrile

A mixture of 3-(4-chlorophenyl)-3-oxopropanenitrile (1.79 g, 10 mmol), 4-chlorobenzaldehyde (0.56 g, 4 mmol) and ammonium acetate (3.08 g, 40 mmol) in 50 ml of glacial acetic acid was heated for 12 h at 120°C under argon atmosphere. After

12 h, sodium nitrite (2.76 g, 40 mmol) was added in portions to a suspension under stirring at 60-70°C. The mixture was stirred for 1 h at the same temperature. After cooled down to room temperature, the mixture was then diluted with 200 mL ice-water mixture, and neutralized with ammonia. The precipitate was filtered off and wash with water to afford 2,4,6-tris(4-chlorophenyl)pyridine-3,5-dicarbonitrile as white powder (1.37 g, yield: 85%). ^{1}H NMR ($CDCl_3$, 400 MHz) δ (ppm):7.54-7.57 (m, 6H), 7.61-7.63 (m, 2H), 8.00-8.04 (m, 4H). ^{13}C NMR ($CDCl_3$, 100 MHz) δ (ppm): 105.8, 115.5, 116.4, 129.3, 129.7, 130.3, 130.9, 131.6, 134.4, 137.9, 138. HRMS (ESI): m/z $[M+H]^+$ calcd for $C_{25}H_{12}Cl_3N_3^+$: 460.0170; found: 460.0164.

Synthesis of 2,4,6-tris(4-(10*H*-phenoxazin-10-yl)phenyl)pyridine-3,5-dicarbonitrile (tri-PXZ-PCN)

2,4,6-tris(4-chlorophenyl)pyridine-3,5-dicarbonitrile (1.04 g, 2.25 mmol), phenoxazine (1.5 g, 8.2 mmol), sodium tert-butoxide (787 mg, 8.2 mmol), palladium (II) acetate (22 mg, 0.1 mmol) and tri-tert-butylphosphine tetrafluoroborate (119 mg, 0.41 mmol) were added to a dry two-necked flask equipped with a magnetic stir bar and a condenser. The flask was then evacuated and backfilled with argon, this evacuation and backfill procedure was repeated twice. Then 20 mL toluene was added under argon atmosphere. The mixture was then stirred under reflux at 110°C for 24 h. As the mixture was cooled down to room temperature, the reaction solution was transferred into a separatory funnel and then neutralized with anhydrous sodium sulfate. The organic phase was dried over anhydrous sodium sulfate (Na_2SO_4), After filtration and concentration under reduced pressure, the crude product was purified by column chromatography with

dichloromethane/petroleum ether (v/v=1/1) as eluent to give the title compound as red powder (1.64 g, yield: 81%). The resulting product was further purified by recrystallizing from a mixture of chloroform/hexane. Finally, this material was purified by sublimation under reduced pressure for OLED fabrication. ^{1}H NMR ($CDCl_3$, 400 MHz) δ (ppm): 6.07 (d, J = 8.0 Hz, 6H), 6.62-6.76 (m, 18H), 7.62 (d, J = 8.0 Hz, 4H), 7.69 (d, J = 12.0 Hz, 2H), 7.91 (d, J = 8.0 Hz, 2H), 8.38 (d, J = 8.0 Hz, 4H). ^{13}C NMR ($CDCl_3$, 100 MHz) δ (ppm): 106.3, 113.5, 115.5, 115.8, 121.97, 122.01, 123.4, 123.5, 131.5, 131.8, 131.9, 132.4, 133.3, 133.7, 135.9, 142.1, 142.5, 144.0, 160.0, 162.3. HRMS (ESI): m/z $[M+H]^+$ calcd for $C_{61}H_{37}N_6O_3^+$: 901.2922; found: 901.2923.

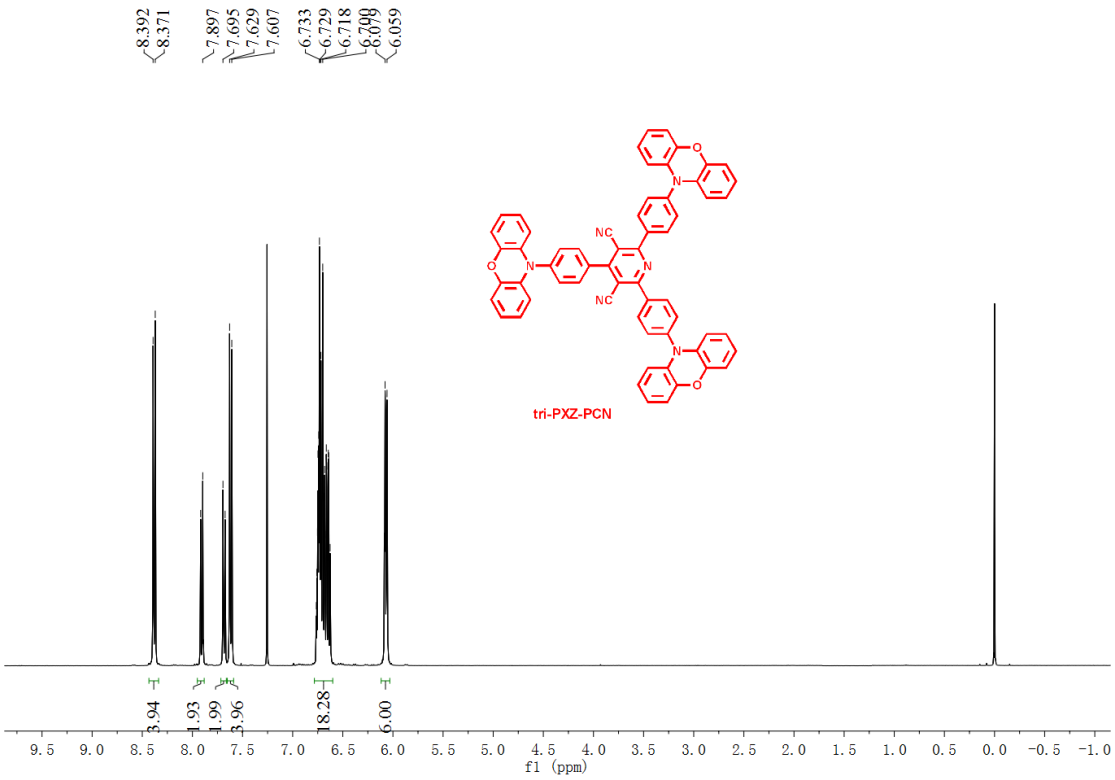

Figure S5. ^{1}H NMR spectrum of tri-PXZ-PCN in $CDCl_3$ (400 MHz, 25 ^{o}C).

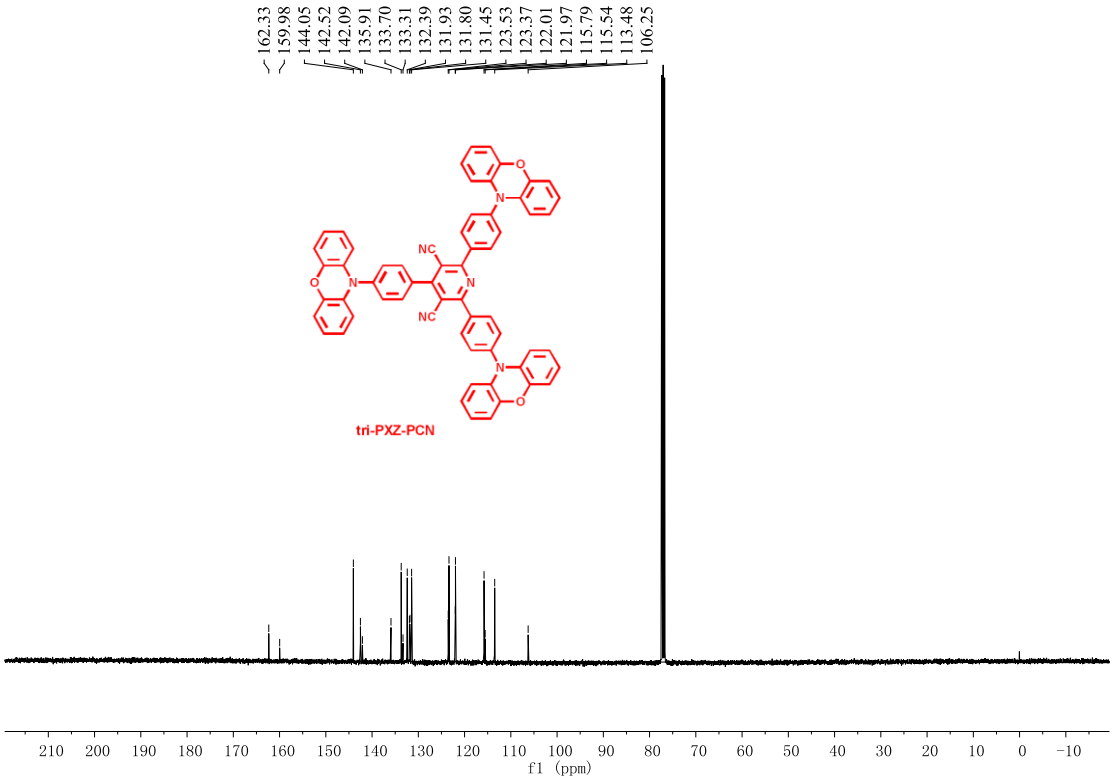

Figure S6. ^{13}C NMR spectrum of bis-PXZ-PCN in $CDCl_3$ (100 MHz, 25 ºC).

Table S1. Crystallographic data summary of PXZ-PCN and bis-PXZ-PCN

	PXZ-PCN	**bis-PXZ-PCN**
CCDC	1821566	1821567
Empirical formula	$C_{37}H_{22}N_4O$	$C_{49}H_{29}N_5O_2$, 3($CHCl_3$)
Formula weight	538.59	1077.88
T (K)	296	296
a (Å)	19.964 (2)	10.3134 (9)
b (Å)	13.6664 (14)	13.439 (1)
c (Å)	20.645 (2)	18.0482 (15)
α (º)	90	80.535 (9)

β (°)	90	88.487 (3)
γ (°)	90	83.795 (3)
V (Å^3), Z	5632.7 (10), 8	2452.9 (3)
R_1, wR_2 [I>2σ(I)]	0.0524, 0.1496	0.1318, 0.4173
Goodness-of-fit on F^2	0.978	1.204

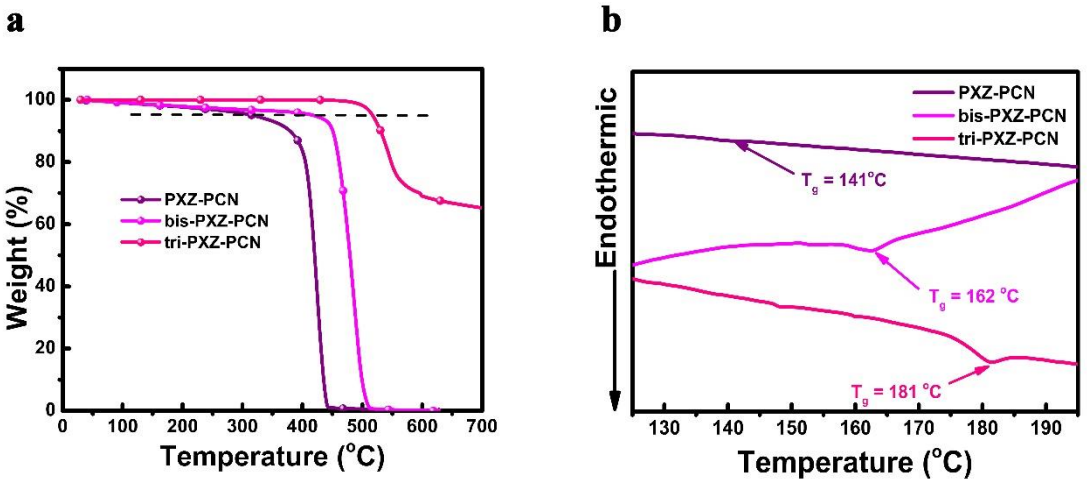

Figure S7. TGA curves (**a**) and DSC curves (**b**) of PXZ-PCN, bis-PXZ-PCN and tri-PXZ-PCN

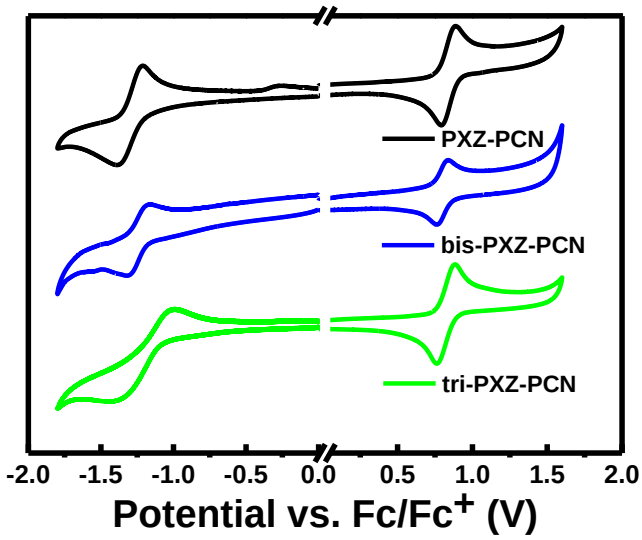

Figure S8. Cyclic voltammograms of PXZ-PCN, bis-PXZ-PCN and tri-PXZ-PCN in 0.1 M $TBAPF_6$ dichloromethane (for the oxidation process) and THF or acetonitrile (for the reduction process) solutions at a scan rate of 50 and 100 $mV \cdot s^{-1}$, respectively.

Table S2. Thermal, electrochemical and TD-DFT calculation data of the three compounds

Compound	HOMO[a]/LUMO[b][eV]	HOMO[c]/LUMO[c][eV]	T_g[d]/T_m[d]/T_d[e][°C]
PZX-PCN	-5.13/-3.09	-4.65/-2.51	141/306/318
bis-PXZ-PCN	-5.11/-3.27	-4.79/-2.66	162/344/418
tri-PXZ-PCN	-5.13/-3.23	-4.75/-2.77	181/389/517

[a] Obtained from cyclic voltammograms in CH_2Cl_2 solution for oxidation. [b] Obtained from cyclic voltammograms in THF or CH_3CN solution for reduction. [c] Estimated from DFT calculations. [d] Obtained from DSC measurements. [e] Obtained from TGA measurements (T_d, corresponding to 5% weight loss).

The rate constants of ISC (k_{ISC}) and RISC (k_{RISC}) of three emitters based on the following equations:

$$k_{\mathrm{p}} = \frac{1}{\tau_{\mathrm{p}}} \tag{1}$$

$$k_{\mathrm{d}} = \frac{1}{\tau_{\mathrm{d}}} \tag{2}$$

$$k_{\mathrm{r,s}} = \Phi_{\mathrm{p}} k_{\mathrm{p}} + \Phi_{\mathrm{d}} k_{\mathrm{d}} \approx \Phi_{\mathrm{p}} k_{\mathrm{p}} \tag{3}$$

$$k_{\mathrm{RISC}} \approx \frac{k_{\mathrm{p}} k_{\mathrm{d}} \Phi}{k_{\mathrm{r,s}}} \tag{4}$$

$$k_{\mathrm{ISC}} \approx \frac{k_{\mathrm{p}} k_{\mathrm{d}} \Phi_{\mathrm{d}}}{k_{\mathrm{RISC}} \Phi_{\mathrm{p}}} \tag{5}$$

In this study, the prompt PLQY (Φ_p) and delayed PLQY (Φ_d) were determined by using the total PLQY and the integrated intensity ratio between prompt and delayed components which was calculated from transient photoluminescence measurements. The intensity ratio between prompt (r_p) and delayed (r_d) components were determined using two fluorescent lifetimes (τ_p, τ_d) and fitting parameter (A_p, A_d) as follow.

$$I(t) = A_{\mathrm{p}} e^{-\frac{t}{\tau_p}} + A_{\mathrm{d}} e^{-\frac{t}{\tau_d}} \tag{6}$$

$$r_p = \frac{A_{\mathrm{p}} \tau_{\mathrm{p}}}{A_{\mathrm{p}} \tau_{\mathrm{p}} + A_{\mathrm{d}} \tau_{\mathrm{d}}} \tag{7}$$

$$r_d = \frac{A_{\mathrm{d}} \tau_{\mathrm{d}}}{A_{\mathrm{p}} \tau_{\mathrm{p}} + A_{\mathrm{d}} \tau_{\mathrm{d}}} \tag{8}$$

Then, the prompt PLQY (Φ_p) and delayed PLQY (Φ_d) were determined using intensity ratio (r_p, r_d) and total PLQY.

$$\Phi_{\mathrm{total}} = \Phi_{\mathrm{p}} + \Phi_{\mathrm{d}} \tag{9}$$

$$\Phi_{\mathrm{p}} = r_p \Phi_{\mathrm{total}} \tag{10}$$

$$\Phi_{\mathrm{d}} = r_d \Phi_{\mathrm{total}} \tag{11}$$

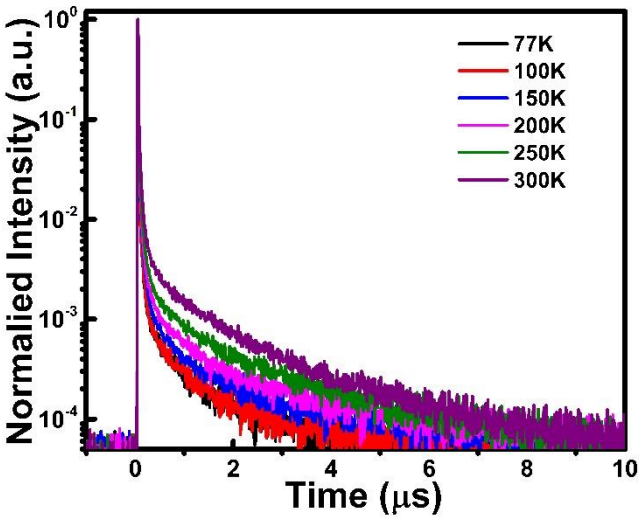

Figure S9. Emission decay profiles of PXZ-PCN doped into CBP films (10 wt%) measured at various temperatures.

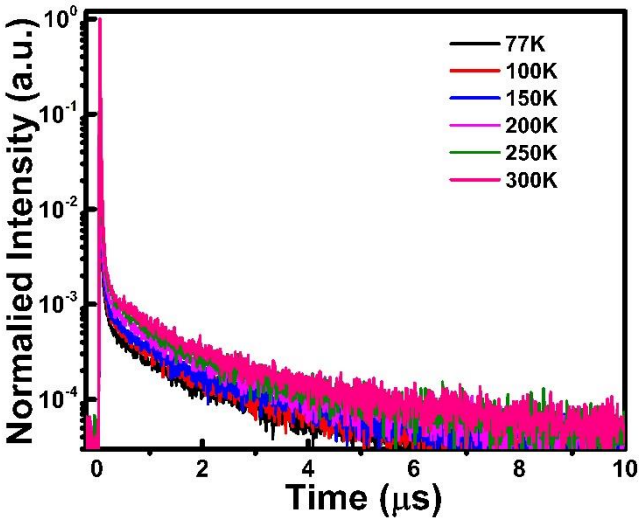

Figure S10. Emission decay profiles of tri-PXZ-PCN doped into CBP films (10 wt%) measured at various temperatures.

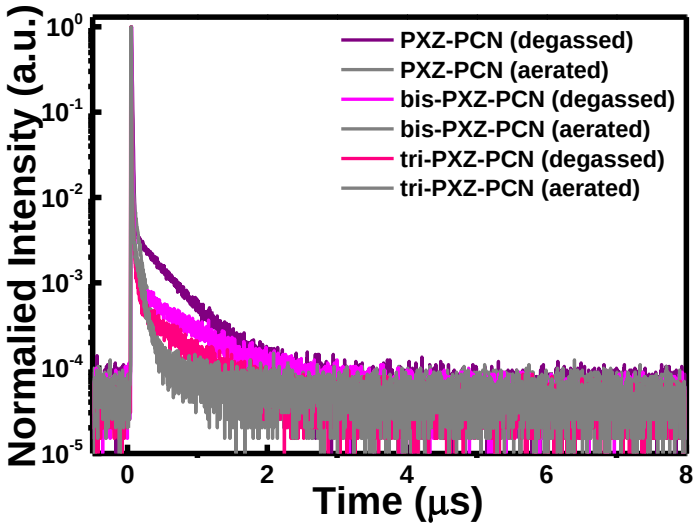

Figure S11. Emission decay profiles for 10^{-4} M toluene solutions of PXZ-PCN, bis-PXZ-PCN and tri-PXZ-PCN at room temperature. The excitation wavelength was 377 nm and the decay curves were measured at 616 nm, 640 nm and 649 nm for PXZ-PCN, bis-PXZ-PCN and tri-PXZ-PCN, respectively.

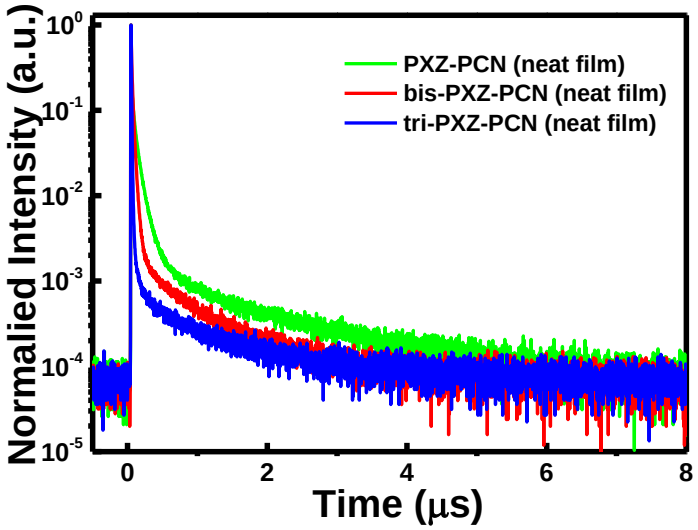

Figure S12. Transient PL characteristics of PXZ-PCN, bis-PXZ-PCN and tri-PXZ-PCN in a neat film at room temperature in Ar (excited at 377 nm).

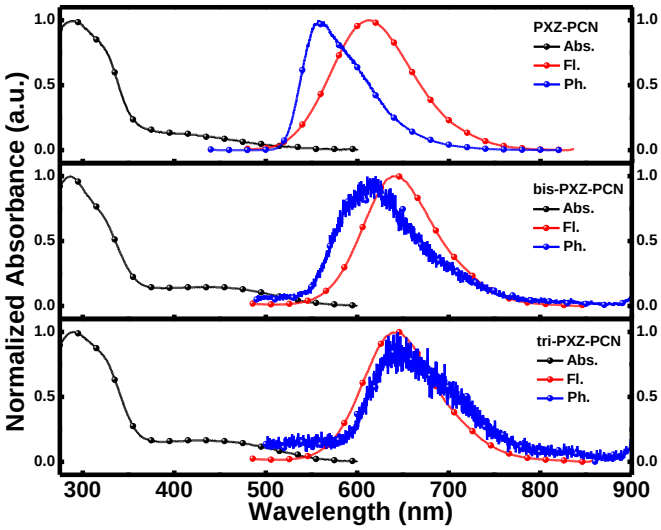

Figure S13. The UV-Vis absorption curves, fluorescence at room temperature and phosphorescence spectra at 77K of PXZ-PCN, bis-PXZ-PCN and tri-PXZ-PCN in neat film.

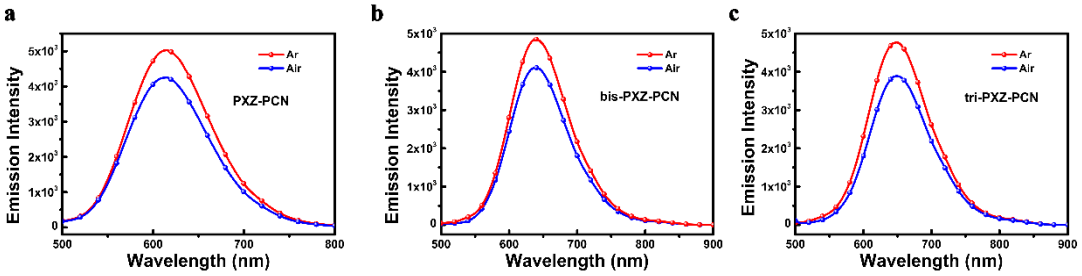

Figure S14. PL spectra of 10^{-4} M PXZ-PCN (a), bis-PXZ-PCN (b) and tri-PXZ-PCN (c) in toluene under air and argon.

Table S3. The summary of the photophysical properties of PXZ-PCN, bis-PXZ-PCN and tri-PXZ-PCN in neat film.

	PXZ-PCN	**bis-PXZ-PCN**	**tri-PXZ-PCN**
$\lambda_{abs,\max}$ (nm)	383	442	435

$\lambda_{em,max}$ (nm)	614	635	645
S_1[a][eV]	2.34	2.17	2.16
T_1[a][eV]	2.39	2.28	2.13
ΔE_{ST}[a] [eV]	0.05	0.11	0.03
τ_{PF}[b] (ns)	54.4	18.7	4.5
τ_{DF}[b] (ns)	726	483	557
Φ_{PL}[c] [%, aerated]	47.5	34.4	26.5

[a] Singlet (S_1) and triplet (T_1) energies were estimated from onsets of the fluorescence and phosphorescence spectra of the three emitters in neat film, respectively. [b] The prompt and delayed fluorescence lifetimes of the investigated molecules in neat film. [c] Absolute PL quantum yields for the investigated molecules doped into CBP (5 wt%). The measurement were conducted with an integrating sphere under air condition at room temperature.

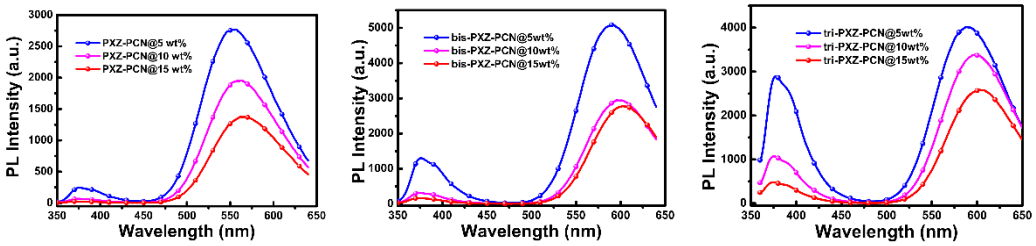

Figure S15. Fluorescence spectra of the three emitters doped in CBP films with different doping concentrations (5wt%, 10wt% and 15wt%).

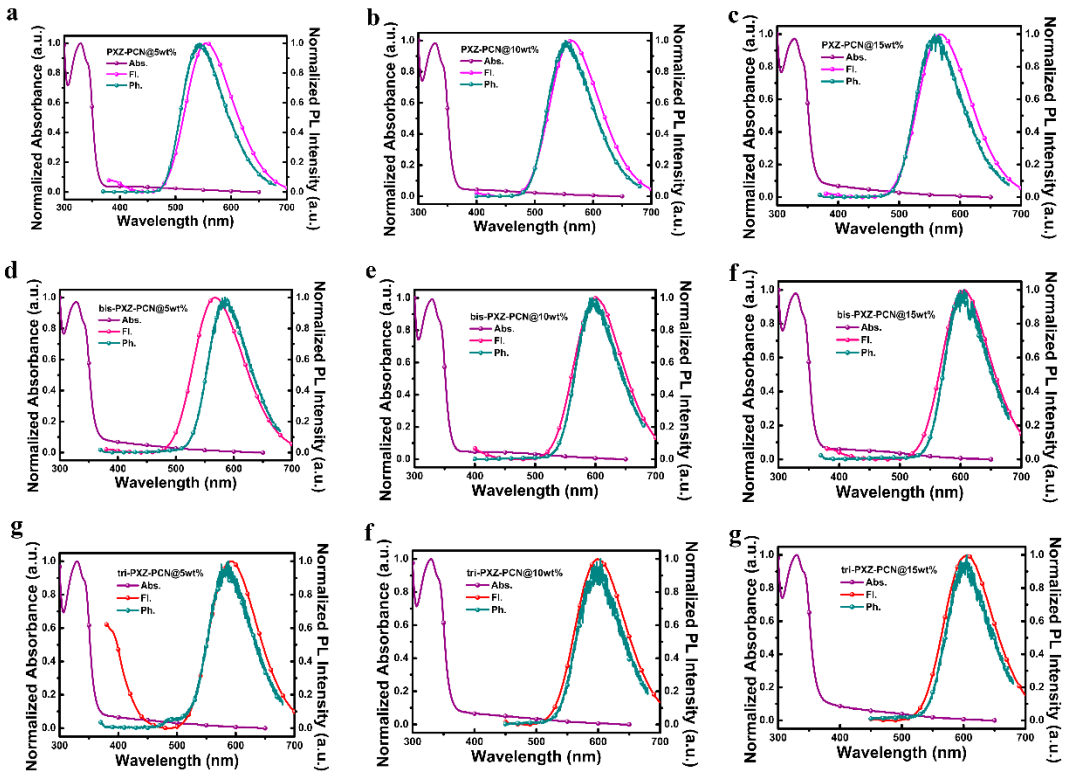

Figure S16. Normalized UV-Vis absorption spectra, fluorescence spectra (both measured at room temperature) and phosphorescence spectra (measured at 77 K) of the three emitters doped in CBP films with different doping concentrations (5wt%, 10wt% and 15wt%).

Table S4. Photophysical data for the three emitters doped in CBP films with different doping concentrations (5wt%, 10wt% and 15wt%).

Doped CBP film	$\lambda_{em,max}$ (nm)	S_1[a](eV)	T_1[a](eV)	ΔE_{ST}[a] (eV)	Φ_{PL}[b](%)
PXZ-PCN@5wt%	557	2.54	2.55	-0.01	65
PXZ-PCN@10wt%	565	2.53	2.52	0.01	57
PXZ-PCN@15wt%	567	2.51	2.50	0.01	51
bis-PXZ-PCN@5wt%	568	2.49	2.36	0.13	43
bis-PXZ-PCN@10wt%	601	2.34	2.30	0.04	36
bis-PXZ-PCN@15wt%	607	2.32	2.28	0.04	31
tri-PXZ-PCN@5wt%	592	2.38	2.37	0.01	43
tri-PXZ-PCN@10wt%	606	2.34	2.29	0.05	34

tri-PXZ-PCN@15wt%	608	2.33	2.27	0.06	29

[a] Experimental data were determined from onsets of the fluorescence and phosphorescence spectra of the three emitters doped into CBP films with different doping concentrations (5wt%, 10wt% and 15wt%). [b] Absolute PL quantum yields for the investigated molecules doped into CBP with different doping concentrations (5wt%, 10wt% and 15wt%) evaluated using an integrating sphere under oxygen-free conditions at room temperature.

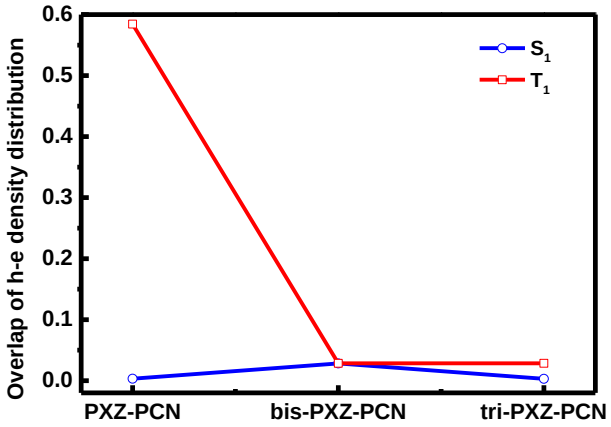

Figure S17. Overlaps between the hole-electron (h-e) density distribution in the adiabatic S_1 and T_1 states.

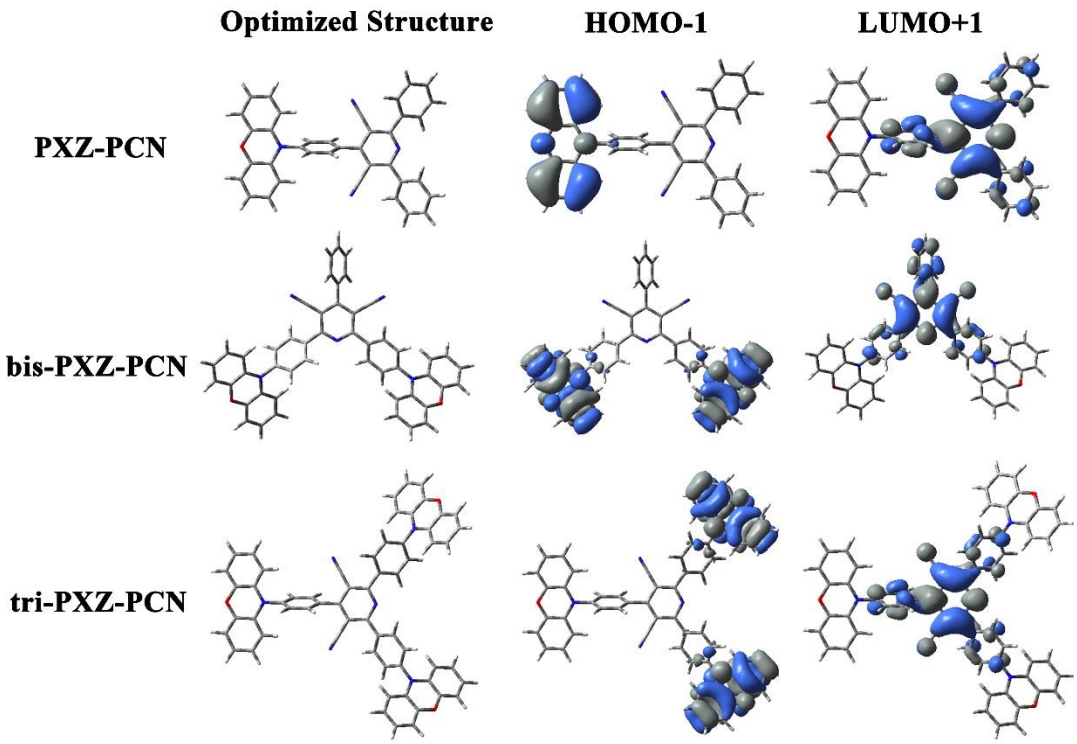

Figure S18. HOMO-1 and LUMO+1 of PXZ-PCN, bis-PXZ-PCN and tri-PXZ-PCN in their S_0 state, as calculated at the B3LYP/6-31G(d) level of theory.

Table S5. Calculated fluorescence oscillator strengths ($f_{S1\rightarrow S0}$), transition dipole moments ($\mu_{S1\text{-}S0}$) and main electron configurations in the adiabatic S_1 states.

Compound	$f_{S1\rightarrow S0}$	$\mu_{S1\text{-}S0}$ [Debye]	Electron configurations
PXZ-PCN	0.0001	6.9271	H→L: 97%
bis-PXZ-PCN	0.0004	0.9805	H→L: 83%
tri-PXZ-PCN	0.0004	3.6018	H→L: 98%

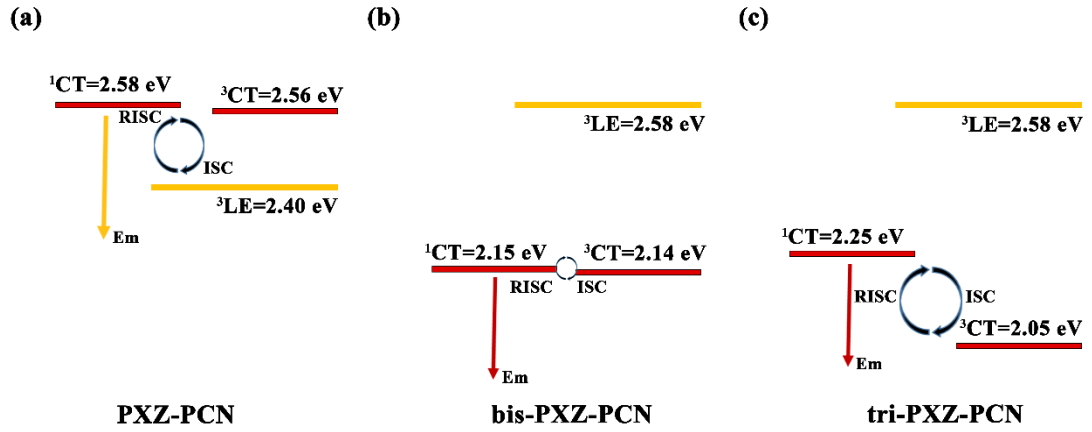

Figure S19. The model for the TADF mechanism in PXZ-PCN (a), bis-PXZ-PCN (b) and tri-PXZ-PCN (c), which considers the ISC and RISC between S_1 and T_1 based on the.

Table S6. Calculated zero-zero energies ($E_{0\text{-}0}$) of the investigated molecules, as calculated by the LC-ωPBE/6-31G(d) level of theory.

Compound	$E_{0\text{-}0}(^1\text{CT})$ (eV)	$E_{0\text{-}0}(^3\text{CT})$ (eV)	$E_{0\text{-}0}(^3\text{LE})$ (eV)	$E_{0\text{-}0}(^3\text{LE}) - E_{0\text{-}0}(^1\text{CT})$ (eV)
PXZ-PCN	2.58	2.56	2.40	-0.18
bis-PXZ-PCN	2.15	2.14	2.58	0.43
tri-PXZ-PCN	2.25	2.05	2.58	0.33

Compared to PXZ-PCN and tri-PXZ-PCN, a decrease in the h/e overlaps of the S_1 and T_1 states for bis-PXZ-PCN leads to a decrease in ΔE_{ST} and hence a slower efficiency roll-off in the device.

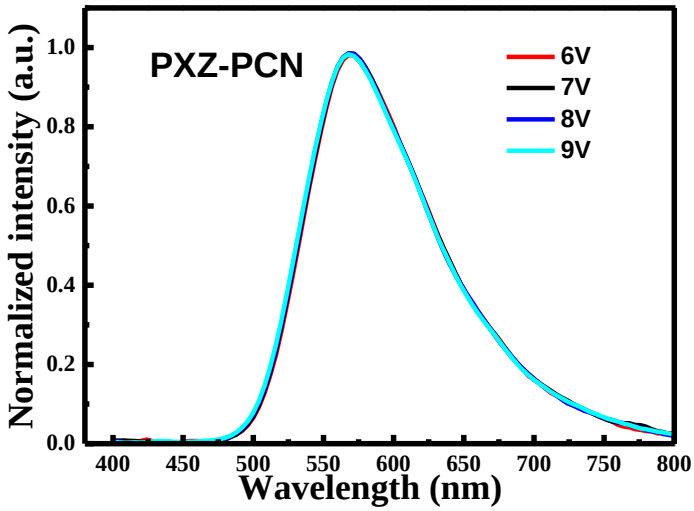

Figure S20. EL spectra of PXZ-PCN under different voltage (CBP as host material).

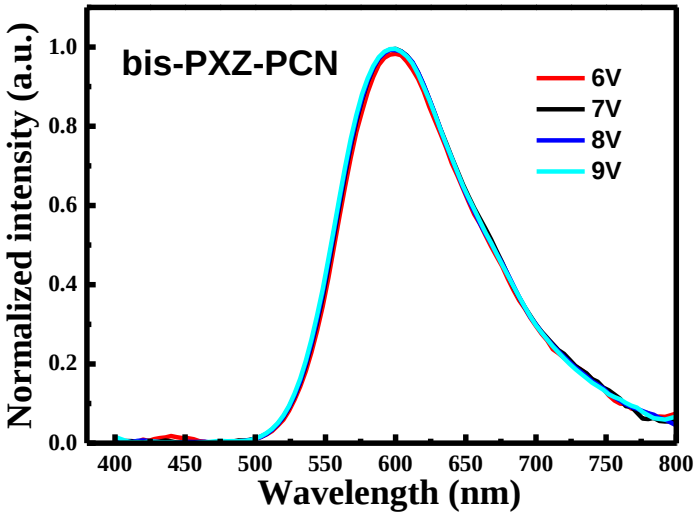

Figure S21. EL spectra of bis-PXZ-PCN under different voltage (CBP as host material).

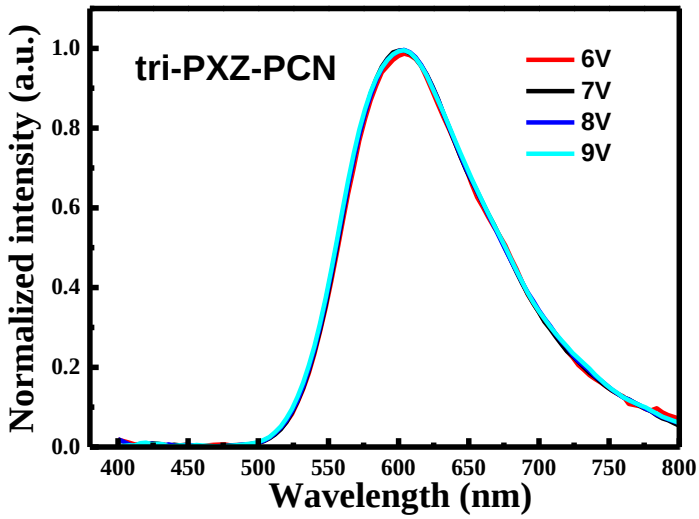

Figure S22. EL spectra of tri-PXZ-PCN under different voltage (CBP as host material).

Reference:

1. T. A. Lin, T. Chatterjee, W. L. Tsai, W. K. Lee, M. J. Wu, M. Jiao, K. C. Pan, C. L. Yi, C. L. Chung, K. T. Wong and C. C. Wu, *Adv. Mater.*, 2016, **28**, 6976.

2. W. M. Wan, A. W. Baggett, F. Cheng, H. Lin, S. Y. Liu and F. Jäkle, *Chem. Commun.*, 2016, **52**, 13616.

3. H. Wang, L. Xie, Q. Peng, L. Meng, Y. Wang, Y. Yi and P. Wang, *Adv. Mater.*, 2014, **26**, 5198.